Soluble VEGF isoforms are essential to establish epiphyseal vascularization and regulate chondrocyte development and survival

Christa Maes, Ingrid Stockmans, Karen Moermans, Riet Van Looveren, Nico Smets, Peter Carmeliet, Roger Bouillon, and Geert Carmeliet

Supplementary references

S1. Carmeliet, P., et al. 1999. Impaired myocardial angiogenesis and ischemic cardiomyopathy in mice lacking the vascular endothelial growth factor isoforms VEGF164 and VEGF188. *Nat. Med.* **5**:495–502.

S2 Decallonne, B., et al. 2000. Streptococcal wall component OK432 restores sensitivity of non-obese diabetic (NOD) thymocytes to apoptotic signals. *Diabetologia.* **43**:1302–1308.

SUPPLEMENTARY DATA

Supplementary Methods

Histomorphometric analysis. Histomorphometric analysis was conducted using a Kontron Electronik image analyzing system (KS400 V 3.00) essentially as described previously in the article. Mineralization and vascularization parameters were quantified on P1.5 tibia sections stained by Von Kossa and CD31, respectively. Trabecular bone volume (as a percentage of tissue volume), capillary density (number of blood vessels per square millimeter) and intercapillary distance (in micrometers) were determined in a defined area of the proximal metaphysis. Capillary invasion of the growth plate was expressed as the number of blood vessels at the metaphyseal growth plate border divided by its width. TRAP-positive cell density was determined in a defined area of the P1.5 proximal tibia. Measurements of tibia length, bone marrow cavity length, and growth plate characteristics were done at three sites, equally distributed along the width of the proximal growth plate. When required, the lateral and central growth plate regions were analyzed separately.

Analysis by qRT-PCR. Analysis using qRT-PCR was performed with specific primers and probes for Ihh, PTHrP, MMP-13, MT1-MMP, RANK, HIF-1α, HIF-2α, $VEGF_{164}$, $VEGF_{188}$ (Table S2), Flt-1, Flk-1, NRP-1 (S1), $VEGF_{120}$, total VEGF, Cbfa-1, osteocalcin, MMP-9 (see article ref. 9), Bcl-2, and Bax (S2). Expression levels were normalized for HPRT expression (S1).

Generation of $VEGF^{120/188}$ and $VEGF^{164/188}$ mice. $VEGF^{120/188}$ mice (expressing both $VEGF_{120}$ and $VEGF_{188}$) or $VEGF^{164/188}$ mice (expressing both $VEGF_{164}$ and $VEGF_{188}$), taken together with WT littermates (i.e., $VEGF^{+/+}$ mice expressing all three isoforms) were obtained by crossing heterozygous $VEGF^{120/+}$ mice (S1) or $VEGF^{164/+}$ mice, respectively, with $VEGF^{188/+}$ mice. Genotyping was performed by double PCR reactions.

Supplementary Results

Reduced growth and skeletal development in $VEGF^{188/188}$ mice. $VEGF^{188/188}$ mice were considerably smaller and had reduced body weights as compared with WT animals throughout embryonic development and postnatal life (see Supplementary Figure 1a).

A severe delay in development of long bones was already observed at E16.5, as evidenced by the reduced area of cartilage resorption (length of primitive bone marrow cavity relative to total tibia length was reduced 80%, $P < 0.0001$; see Supplementary Figure 1, b and c).

Metaphyseal vascularization, mineralization, and resorption are normal in $VEGF^{188/188}$ mice.

Metaphyseal vascularization in $VEGF^{188/188}$ mice was normal, as analyzed by immunohistochemical staining for CD31 on P1.5 bone sections. The degree and pattern of the vascular invasion at the growth plate, the vascular density, and the intercapillary distance in the bone region underneath the growth plate were similar in $VEGF^{188/188}$ and WT tibias (Supplementary Table 1). Concomitantly, trabecular bone volume and osteocalcin expression was normal in $VEGF^{188/188}$ mice (see Supplementary Table 1). Expression levels of several MMPs (MMP-9, MMP-13, and MT1-MMP) and the osteoclast marker RANK were normal, and no significant alterations were found in the number of TRAP-positive cells in $VEGF^{188/188}$ bones (see Supplementary Table 1). These data indicate that metaphyseal vascularization, bone mineralization, and resorption parameters were normal in $VEGF^{188/188}$ mice, indicating that the abnormalities were restricted to the epiphysis. Metaphyseal vascularization and mineralization were also normal in $VEGF^{164/164}$ mice (not shown).

Histological examination of $VEGF^{120/188}$ and $VEGF^{164/188}$ mice. To further elucidate whether the phenotype of the $VEGF^{188/188}$ mice was due to inactivation of the $VEGF_{120}$ and/or the $VEGF_{164}$ isoform, we generated mice expressing $VEGF_{120}$ or $VEGF_{164}$ in addition to $VEGF_{188}$ ($VEGF^{120/188}$ and $VEGF^{164/188}$ mice, respectively).

Histological analysis of mice expressing the $VEGF_{164}$ isoform, either exclusively ($VEGF^{164/164}$ mice) or together with $VEGF_{188}$ ($VEGF^{164/188}$ mice), showed no bone, cartilage, or joint phenotype (data not shown), indicating that this isoform can provide the required signals for both vascularization and chondrocyte development.

$VEGF^{120/188}$ mice (n = 3) at P10.5 showed normal development of the knee joint, including the cruciate ligaments, as judged by histological criteria. The formation of the secondary ossification centers also appeared to occur largely normal in $VEGF^{120/188}$ mice —

although a slight delay as compared with WT cannot be excluded — suggesting that epiphyseal vascularization was not impaired.

All *VEGF*$^{120/188}$ mice, however, displayed an abnormal region located in the center of the epiphysis of the distal femur, at a site that becomes substantially hypoxic during normal development (article ref. 2) (Supplementary Figure 2a). This region largely consisted of acellular matrix, the morphology of which was highly similar to the remnants of the apoptotic chondrocytes seen in the lesion of *VEGF*$^{188/188}$ mice (Supplementary Figure 2b). This observation suggests impaired survival of hypoxic chondrocytes in mice coexpressing $VEGF_{120}$ and $VEGF_{188}$, supporting the crucial role of the $VEGF_{164}$ isoform as a survival factor.

These data indicate that the *VEGF*$^{188/188}$ phenotype can be partially rescued by additional expression of the $VEGF_{120}$ isoform, but that a complete prevention of chondrocyte cell death requires (co-)expression of $VEGF_{164}$.

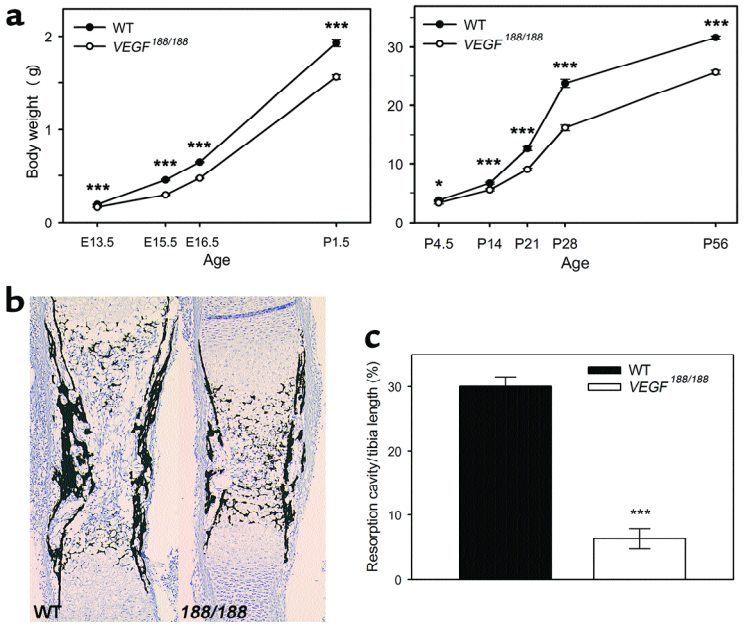

Figure 1
Impaired growth and delayed bone development in *VEGF*$^{188/188}$ mice. (**a**) Body weights of WT and *VEGF*$^{188/188}$ mice as a function of age, both at embryonic stages and throughout postnatal life. (**b**) Histological sections of E16.5 WT and *VEGF*$^{188/188}$ tibias stained with Von Kossa and hematoxylin, showing delayed bone development in *VEGF*$^{188/188}$ mice, as evidenced by significant reduced bone marrow cavity length (**c**). Values are means ± SEM, $*P < 0.05$; $***P < 0.001$ (*t* test).

Figure 2
Incomplete rescue of the *VEGF*$^{188/188}$ phenotype by additional expression of the $VEGF_{120}$ isoform (*VEGF*$^{120/188}$ mice). (**a**) Histological analysis of H&E stained longitudinal sections through the knee, showing femur (right) and tibia (left) of WT and *VEGF*$^{120/188}$ mice at P10.5. The cruciate ligaments appear morphologically similar in both genotypes, and the formation of the secondary ossification centers (marked by red linings) seems to occur largely normal in *VEGF*$^{120/188}$ mice, except for a possible slight delay as compared with WT. An abnormal epiphyseal region is, however, noted in the lower center of the femur in the mutants (arrowheads). (**b**) Higher magnification of this femoral epiphyseal region of *VEGF*$^{120/188}$ mice, showing that it largely consists of acellular matrix. This morphology is highly similar to the remnants of the apoptotic chondrocytes seen in the lesion of *VEGF*$^{188/188}$ mice (inset shows *VEGF*$^{188/188}$ femur at P5). Scale bars: (**a**) 500 μm; (**b**) 100 μm.

Table 1
Histomorphometric and quantitative RT-PCR analysis of metaphyseal bone vascularization, mineralization, and resorption parameters

Parameter	WT	*VEGF*$^{188/188}$
Vascularization[A]		
Capillary invasion at growth plate	11.8 mm^{-1} ± 0.4 (n = 6)	10.8 mm^{-1} ± 0.6 (n = 10)
Capillary density	95.1 mm^{-2} ± 3.5 (n = 6)	93.8 mm^{-2} ± 3.9 (n = 9)
Intercapillary distance	92 μm ± 3 (n = 6)	97 μm ± 5 (n = 10)
Mineralization		
TBV[A]	18.3% ± 2.2% (n = 5)	17.5% ± 0.8% (n = 5)
Osteocalcin mRNA[B]	100% ± 23%	101% ± 18%
Resorption		
MMP-9 mRNA[B]	100% ± 9%	111% ± 14%
MMP-13 mRNA[B]	100% ± 10%	80% ± 6%
MT1-MMP mRNA[B]	100% ± 5%	87% ± 7%
RANK mRNA[B]	100% ± 14%	88% ± 12%
TRAP-positive cell density[A]	15.2% ± 1.7% (n = 4)	14.4% ± 4.0% (n = 10)

[A]Metaphyseal vascularization parameters, TBV, and TRAP-positive cell density were determined in the proximal tibia of sections stained for CD31, Von Kossa, or TRAP, respectively, using an image analysis system. [B]Number of mRNA copies relative to HPRT copy number was determined by qRT-PCR of WT and mutant femurs at P1.5, as described in Methods. WT values were set at 100%. No significant differences were found between the mutant and WT genotypes. TBV, trabecular bone volume.

Table 2
Oligonucleotide sequences used in qRT-PCR

Gene		Sequence
Ihh	F	5′-TCCCGACATCATCTTCAAGGA-3′
	R	5′-GGCCACTGGTTCATGACAGA-3′
	P	5′-FAM-AACACGGGTGCCGACCGCC-TAMRA-3′
PTHrP	F	5′-TTAGAGGCGCTGATTCCTACACA-3′
	R	5′-CACGGAGTAGCTGAGCAGGAATA-3′
	P	5′-FAM-CCAGAGCCAGCGAGCGGCAC-TAMRA-3′
MMP-13	F	5′-ACTTCTACCCATTTGATGGACCTT-3′
	R	5′-AAGCTCATGGGCAGCAACA-3′
	P	5′-FAM-CACACGCTTTTCCTCCTGGACCAAACT-TAMRA-3′
MT1-MMP	F	5′-TCGTGTTGCCTGATGACGAT-3′
	R	5′-TTTGGGCTTATCTGGGACAGA-3′
	P	5′-FAM-TTTATGGAAGCAAGTCAGGGTCACCCAC-TAMRA-3′
RANK	F	5′-GAGCTCAGCATCCCTTGCA-3′
	R	5′-CCCTGGTGTGCTTCTAGCTTTC-3′
	P	5′-FAM-TCCTGGGCTTCTTCTCAGATGTCTTTTCG-TAMRA-3′
HIF-1α	F	5′-TGAGCTCACATCTTGATAAAGCTTCT-3′
	R	5′-GGGCTTTCAGATAAAAACAGTCCAT-3′
	P	5′-FAM-AGACCACCGGCATCCAGAAGTTTTCTCA-TAMRA-3′
HIF-2α	F	5′-CTCATGTCTCCATGTTCAAGATGA-3′
	R	5′-CATACGTTTCCACATCAAGTGTGA-3′
	P	5′-FAM-TCTTGGAAGGCTTGCTCCTCATACTCCAG-TAMRA-3′
VEGF$_{164}$	F	5′-TGCAGGCTGCTGTAACGATG-3′
	R	5′-GAACAAGGCTCACAGTGATTTTCT-3′
	P	5′-FAM-TGTCTTTCTTTGGTCTGCATTCACATCGG-TAMRA-3′
VEGF$_{188}$[A]	R	5′-CTCCAGGATTTAAACCGGGATT-3′

[A]F and P for amplification of VEGF$_{188}$ were identical to those for amplification of VEGF$_{164}$. F, forward primer; R, reverse primer; P, probe.